Cecropia peltata accumulates starch or soluble glycogen by differentially regulating starch biosynthetic genes

Bischof, Sylvain ; Umhang, Martin ; Eicke, Simona ; Streb, Sebastian ; Qi, Weihong ; Zeeman, Samuel C

Abstract: The branched glucans glycogen and starch are the most widespread storage carbohydrates in living organisms. The production of semicrystalline starch granules in plants is more complex than that of small, soluble glycogen particles in microbes and animals. However, the factors determining whether glycogen or starch is formed are not fully understood. The tropical tree Cecropia peltata is a rare example of an organism able to make either polymer type. Electron micrographs and quantitative measurements show that glycogen accumulates to very high levels in specialized myrmecophytic structures (Müllerian bodies), whereas starch accumulates in leaves. Compared with polymers comprising leaf starch, glycogen is more highly branched and has shorter branches–factors that prevent crystallization and explain its solubility. RNA sequencing and quantitative shotgun proteomics reveal that isoforms of all three classes of glucan biosynthetic enzyme (starch/glycogen synthases, branching enzymes, and debranching enzymes) are differentially expressed in Müllerian bodies and leaves, providing a system-wide view of the quantitative programming of storage carbohydrate metabolism. This work will prompt targeted analysis in model organisms and cross-species comparisons. Finally, as starch is the major carbohydrate used for food and industrial applications worldwide, these data provide a basis for manipulating starch biosynthesis in crops to synthesize tailor-made polyglucans.

DOI: https://doi.org/10.1105/tpc.113.109793

The Plant Cell, Vol. 25: 1400–1415, April 2013, www.plantcell.org

Cecropia peltata Accumulates Starch or Soluble Glycogen by Differentially Regulating Starch Biosynthetic Genes[W][OA]

Sylvain Bischof,[a,1,2] Martin Umhang,[a,1] Simona Eicke,[a] Sebastian Streb,[a] Weihong Qi,[b] and Samuel C. Zeeman[a,3]

[a] Department of Biology, ETH Zurich, 8092 Zurich, Switzerland
[b] Functional Genomics Center Zurich, 8057 Zurich, Switzerland

The branched glucans glycogen and starch are the most widespread storage carbohydrates in living organisms. The production of semicrystalline starch granules in plants is more complex than that of small, soluble glycogen particles in microbes and animals. However, the factors determining whether glycogen or starch is formed are not fully understood. The tropical tree *Cecropia peltata* is a rare example of an organism able to make either polymer type. Electron micrographs and quantitative measurements show that glycogen accumulates to very high levels in specialized myrmecophytic structures (Müllerian bodies), whereas starch accumulates in leaves. Compared with polymers comprising leaf starch, glycogen is more highly branched and has shorter branches—factors that prevent crystallization and explain its solubility. RNA sequencing and quantitative shotgun proteomics reveal that isoforms of all three classes of glucan biosynthetic enzyme (starch/glycogen synthases, branching enzymes, and debranching enzymes) are differentially expressed in Müllerian bodies and leaves, providing a system-wide view of the quantitative programming of storage carbohydrate metabolism. This work will prompt targeted analysis in model organisms and cross-species comparisons. Finally, as starch is the major carbohydrate used for food and industrial applications worldwide, these data provide a basis for manipulating starch biosynthesis in crops to synthesize tailor-made polyglucans.

INTRODUCTION

Glycogen and starch are the most widespread storage carbohydrates in living organisms. Archaea, bacteria, and many eukaryotes (including yeast, fungi, and animals) accumulate glycogen, while plants make starch (Zeeman et al., 2010; Ball et al., 2011). However, there are a few exceptions to this rule, including the fast-growing pioneer tree native to subtropical regions, *Cecropia peltata* (Fleming and Williams, 1990). *C. peltata* is known for its invasive nature (www.issg.org), and its leaf extracts are reported to have medicinal properties effective against rheumatism, malaria, and diabetes (Pérez-Guerrero et al., 2001; Andrade-Cetto and Heinrich, 2005; Uchoa et al., 2010). *C. peltata* has a myrmecophytic lifestyle, sharing a symbiotic relationship with stinging ants (Folgarait et al., 1994; Faveri and Vasconcelos, 2004), which inhabit the hollow trunk and protect the tree against herbivores and competition from vines. The ants feed on Müllerian bodies (MBs) (Müller, 1876), specialized multicellular egg-like bodies produced on a pad of trichome-covered tissue (the trichilium) at the petiole-stem interface (Figure 1). In 1971, Rickson made the remarkable discovery that the MBs accumulate large amounts of a soluble, glycogen-like polysaccharide in 8- to 10-μm diameter plastid-like organelles, while starch is synthesized in leaf chloroplasts (Rickson, 1971).

It has been proposed that the ability of plants to synthesize starch evolved from an ancestral capacity to make glycogen. The known starch biosynthetic enzymes are a mosaic derived from the host and cyanobacterial endosymbiont genomes (Ball and Morell, 2003; Patron et al., 2005; Deschamps et al., 2008). Amylopectin (the major constituent of starch) and glycogen are both composed of α-1,4-linked glucan chains, branched through α-1,6 linkages (Shearer and Graham, 2002; Zeeman et al., 2010). Amylopectin has chains between six and >100 Glc units in length (averaging around 20), with a branch frequency of 4 to 6%. The combination of chain lengths and branching pattern allows neighboring linear chain segments to form double helices, which organize into in radially oriented arrays. This results in concentric, crystalline layers and allows essentially unlimited growth of the insoluble starch granules, which can reach large dimensions (over 100 μm). By contrast, glycogen tends to have shorter chain lengths (on average 11 Glc units) and a higher frequency of branch points (7 to 10%), which are evenly distributed (Sullivan et al., 2010). As glycogen molecules grow, the chain density at the exterior increases such that, at ~25 nm diameter, further growth is limited by steric hindrances (Shearer and Graham, 2002). The branching pattern of glycogen, along with the short chain lengths, prevents the formation of the ordered structures observed in starch granules (Meléndez et al., 1998). Starch also contains a second glucan component, amylose, present in amorphous regions between the crystalline layers of amylopectin. Amylose is smaller than amylopectin and is essentially linear or only lightly branched (<1%).

[1] These authors contributed equally to this work.
[2] Current address: Department of Molecular, Cell, and Developmental Biology, University of California, 610 Charles E. Young Drive East Los Angeles, CA 90095-7239.
[3] Address correspondence to szeeman@ethz.ch.
The author responsible for distribution of materials integral to the findings presented in this article in accordance with the policy described in the Instructions for Authors (www.plantcell.org) is: Samuel C. Zeeman (szeeman@ethz.ch).
[W] Online version contains Web-only data.
[OA] Open Access articles can be viewed online without a subscription.
www.plantcell.org/cgi/doi/10.1105/tpc.113.109793

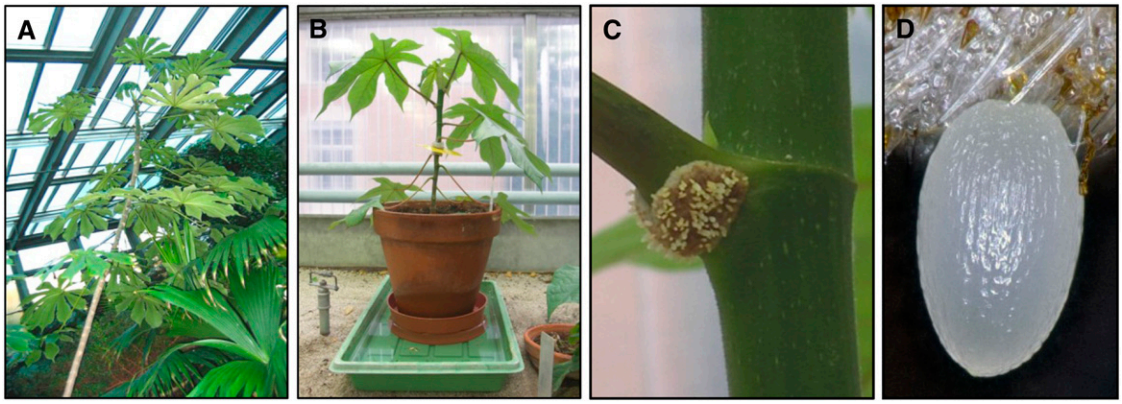

Figure 1. *C. peltata* Produces MBs on Trichilia at the Base of the Petioles.

(A) *C. peltata* tree in the greenhouse. *C. peltata* is a subtropical tree growing up to 20 m within a 20- to 30-year lifespan.
(B) Small *C. peltata* tree obtained by head cuttings.
(C) Trichilium presenting multiple MBs. Trichilia are brownish pads of tissue developing at the abaxial side of the petiole-stem interface of leaves. MBs produced within trichilia emerge through the mat of trichomes.
(D) A single MB emerged from a trichilia. MBs are typically 1 mm wide and 2 mm long.

Unlike amylopectin, amylose is not required for the formation of semicrystalline starch granules (Buléon et al., 1998).

In both glycogen and starch biosynthesis, the substrate is a sugar nucleotide (ADP Glc in green plants and prokaryotes and UDP Glc in red algae, fungi, and animals). The class of enzymes called glycogen/starch synthases transfer activated glucosyl moieties onto the nonreducing ends of existing glucan chains (Shearer and Graham, 2002; Ball and Morell, 2003; Zeeman et al., 2010). In higher plants, five subclasses of starch synthases (SSs) have been studied. Four soluble SSs (SSI, SSII, SSIII, and SSIV) are involved in amylopectin chain elongation. Each has a distinct role, although there is functional overlap between them (Tomlinson and Denyer, 2003; Zhang et al., 2008; Szydlowski et al., 2009). Granule-bound starch synthase (GBSS) synthesizes amylose but may also produce very long amylopectin chains. Concurrent with chain elongation, branching enzymes (BEs) transfer oligosaccharides of six or more Glc units from α-1,4-linked chains, creating an α-1,6 branch point on the same or adjacent chains (Tomlinson and Denyer, 2003). One BE is necessary for glycogen biosynthesis, whereas plants generally have two subclasses, which transfer chains of different lengths. Besides SSs and BEs, debranching enzymes (DBEs) assist in starch biosynthesis by cleaving branch points to facilitate amylopectin crystallization (Zeeman et al., 2010). DBEs fall into two classes: isoamylases (ISAs) and limit dextrinases (also termed pullulanases). Isoamylases can be further subdivided into three subfamilies (ISA1 to ISA3). Studies in several species have implicated ISA1-type DBEs in starch biosynthesis. Its loss results in a dramatic phenotype, with decreased starch and its partial replacement by aberrant water-soluble polyglucans, often referred to as phytoglycogen (Zeeman et al., 2010). However, the severity of this phenotype is variable between species and between cell types within a species. DBEs are also involved in starch breakdown, and ISA3 and limit dextrinase have high activities on glucans with short external chains (Hussain et al., 2003; Delatte et al., 2005; Wattebled et al., 2005; Utsumi and Nakamura, 2006).

To date, substantial work in model organisms provided valuable information on the individual function of the different components involved in carbohydrate metabolism. Nevertheless, it remains unclear how these factors are balanced and work together to regulate and determine the complex architecture of storage polyglucans and, therefore, the capacity to synthesize glycogen or starch. Accumulation of glycogen in the MBs and starch in the leaves of *C. peltata* provides a unique natural system to understand how the carbohydrate biosynthetic machinery can be qualitatively and quantitatively configured to make these two polymer types. To study the molecular features that regulate carbohydrate structure in this nonmodel species, we employed 454 and Illumina sequencing to generate quantitative transcriptional maps of *C. peltata* leaves and MBs. We observed a transcriptional shift of key metabolic genes, aspects of which were confirmed at the protein level by label-free quantitative proteomics. These genome-wide profiling experiments, together with microscopy and biochemical techniques, allow us to understand storage carbohydrate biosynthesis in far greater detail.

RESULTS

MBs of *C. peltata* Accumulate High Amounts of Soluble Sugars and Polyglucans

We first confirmed that the MBs forming on trichilia of *C. peltata* grown in our glasshouses (Figure 1) do indeed contain glycogen-like polyglucans and that the leaves contain starch. Leaf and MB tissue for all experiments were harvested toward the end of the day. Care was taken to collect newly emerged MBs from three active trichilia to ensure they were in a metabolically active state (Figure 1D). Leaf material was taken from the three adjacent leaves. Embedded sections were stained with toluidine

blue for light microscopy. Leaf sections revealed a typical C3 leaf structure with a thick upper epidermal cell layer and a pronounced palisade and spongy mesophyll below (Figure 2A). Ultrastructure was investigated further by transmission electron microscopy. Mesophyll and epidermal cell chloroplasts contained between one and three well-defined discoid starch granules (Figures 2B and 2C) that were comparable in appearance to those seen in other species (e.g., *Arabidopsis thaliana*; Zeeman et al., 2002). No material resembling soluble polysaccharides was detected in chloroplasts.

Light microscopy analysis of transverse sections of MBs (Figure 2D) revealed them to be between 0.5 and 1 mm in diameter. They consisted of homogeneous parenchymal cells covered by a single layer of epidermal cells. Electron micrographs revealed that the parenchymal cells are packed with two types of spherical organelles: ~2-μm diameter electron-transparent lipid droplets (Figure 2E) and ~10-μm diameter organelles surrounded by a double membrane, indicating that they are plastids (Figures 2F and 2G, black arrows). These observations are consistent with those of Rickson (Rickson, 1976a, 1976b), suggesting that the larger spherical organelles are specialized plastids that differentiated from chloroplasts during MB formation. Remnants of an internal membrane system that could have been part of a thylakoid system were visible in some of the MB plastids (Figure 2G, white arrow). Most of the plastid stroma was filled with small electron-dense 20- to 30-nm particles, comparable in size and shape to glycogen particles in animals or phytoglycogen particles accumulating in DBE mutants of *Arabidopsis* (Delatte et al., 2005). No starch granules were detected in any of the MB plastids, neither in the parenchyma cells nor the epidermal cells (Figures 2E to 2G).

To obtain more information on MB carbohydrate metabolism, we extracted soluble sugars and compared the levels with those in leaves harvested at the end of the day. Low molecular weight sugars were analyzed using high-performance anion-exchange chromatography coupled to pulsed-amperometric detection (HPAEC-PAD). Glc, Fru, and Suc levels were all two- to fourfold higher in MBs than in leaves (Figure 3A). Maltose levels were low in leaves but high in MBs (a 280-fold increase). We examined the quantity and nature of the polyglucans (Figure 3A) by analyzing (1) the water-insoluble fraction (i.e., starch), (2) the total water-soluble fraction, and (3) the water-soluble but methanol-precipitable fraction (i.e., glycogen). In leaves, most of the polyglucan was insoluble and the levels were comparable to starch levels in *Arabidopsis* leaves (10 to 15 mg Glc equivalents g^{-1} fresh weight). Although we did not observe any starch-like structures in MBs, they also contained some insoluble polyglucans. The absolute levels were comparable to those of insoluble polyglucans in leaves but very low relative to the extremely high levels of total soluble polyglucans (Figure 3A), which accumulated to between 25 and 33% of the MB fresh weight. The majority (88%) of the soluble polyglucans were precipitable by methanol, suggesting they have a high molecular weight. There were also significant amounts of smaller soluble polyglucans in MBs (12%, corresponding to 37 mg Glc equivalents g^{-1} fresh weight, of maltose and other malto-oligosaccharides). In leaves, small amounts of soluble polyglucan were present, of which 97% were precipitable by methanol. This suggests that large glycogen-like polyglucans might be present in some leaf cells. To characterize the different polyglucan fractions further, we analyzed their structural properties.

MB Glycogen Consists of Short-Chain Highly Branched Polyglucan

Chain length distributions (CLDs) provide insight into branched polyglucan architecture, which determines solubility and crystallization competence (Zeeman et al., 2007). We compared the CLD of leaf starch from *C. peltata* with that of *Arabidopsis* (see Supplemental Figure 1A online). The starches were hydrolyzed with commercial DBEs, and the resulting linear chains were separated and detected by HPAEC-PAD (see Supplemental Methods online). *C. peltata* leaf starch had slightly more chains with a degree of polymerization (DP; the number of glucosyl units comprising a chain) of between 16 and 30 and slightly fewer between DP 5 and 15 compared with *Arabidopsis* leaf starch. Greater differences were observed between the CLDs of soluble MB polyglucans and the starches. Short chains of DP 5 to 10 were increased, and chains of DP 11 to 21 were decreased in the soluble MB polyglucans, compared with the leaf starch (Figure 3B). The small percentages of *C. peltata* leaf polyglucans found in the soluble fraction and MB polyglucans in the insoluble fraction were also analyzed. Interestingly, the soluble leaf polyglucans had a similar CLD to the leaf starch (see Supplemental Figure 1B online). Similarly, the CLDs of the insoluble and soluble MB polyglucans were very similar (see Supplemental Figure 1C online). It is possible that the extraction procedure results in some solubilization of the leaf starch or that tiny leaf starch granules are not easily pelleted in the initial extraction. It is also possible a few MB cells were not lysed during extraction or that there was slight contamination of the MB insoluble fraction by the soluble fraction due to the massive amount of soluble polyglucans present in MBs. In combination with the microscopy analyses (Figure 2), the CLD analyses indicate that only one type of polyglucan is synthesized in either leaves or MBs.

To gain information about the distribution and proximity of internal branch points, we digested outer chains that do not bear a branch point using β-amylases before debranching and HPAEC-PAD analysis (β-CLD; Figure 3C). Chains of DP 2 and 3, originating from digested external chains, were most abundant in the profiles but are not displayed. There were striking differences between the profiles of *C. peltata* leaf starch and MB glycogen (Figure 3C). Internal chains of DP 4 and 5 were the most abundant internal chains in MB glycogen, indicative of branch points that are very close together. By contrast, the β-CLD of leaf starch had many longer chains of DP ≥10, suggesting that the branch points are more widely spaced (for further explanation, see Supplemental Figure 2 online). Collectively, structural analysis using CLD and β-CLD revealed that soluble *C. peltata* MB glycogen is a branched polysaccharide, with shorter chains and branch points closer together, compared with leaf starch, supporting earlier studies (Marshall and Rickson, 1973).

Next-Generation Sequencing of the *C. peltata* Transcriptome

To identify the molecular components responsible for tissue-specific polyglucan synthesis, we generated transcriptional maps

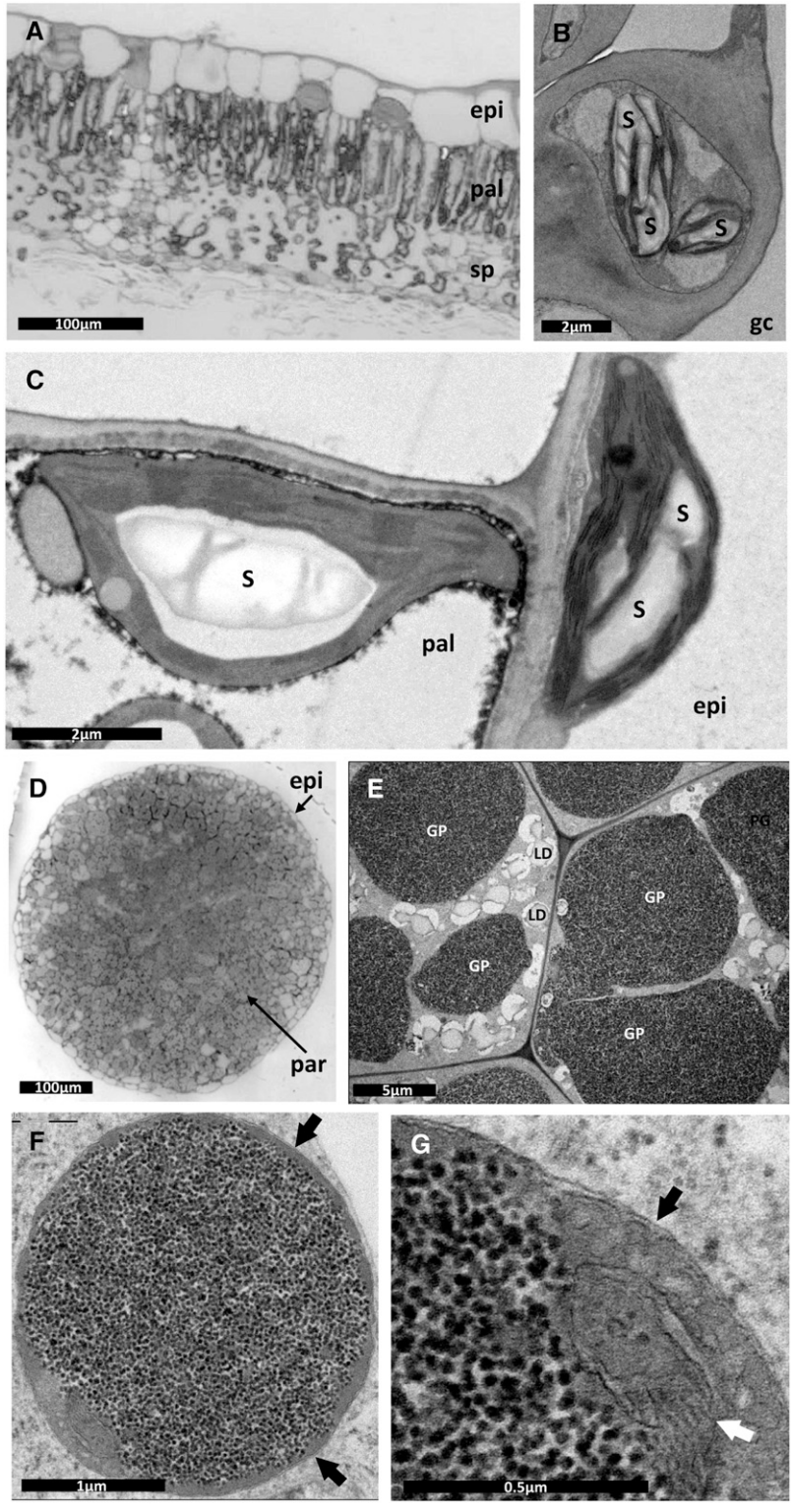

Figure 2. Light and Transmission Electron Microscopy of *C. peltata* Leaves and MBs.

Leaves and MBs were harvested at the end of the day, fixed in glutaraldehyde, and stained using osmium-(VIII)-oxide.
(A) Light microscopy of toluidine blue–stained leaf section containing a thick epidermis (epi), palisade mesophyll (pal), and spongy mesophyll (sp).
(B) Transmission electron micrograph of leaf section showing starch granules (S) inside a guard cell (gc).

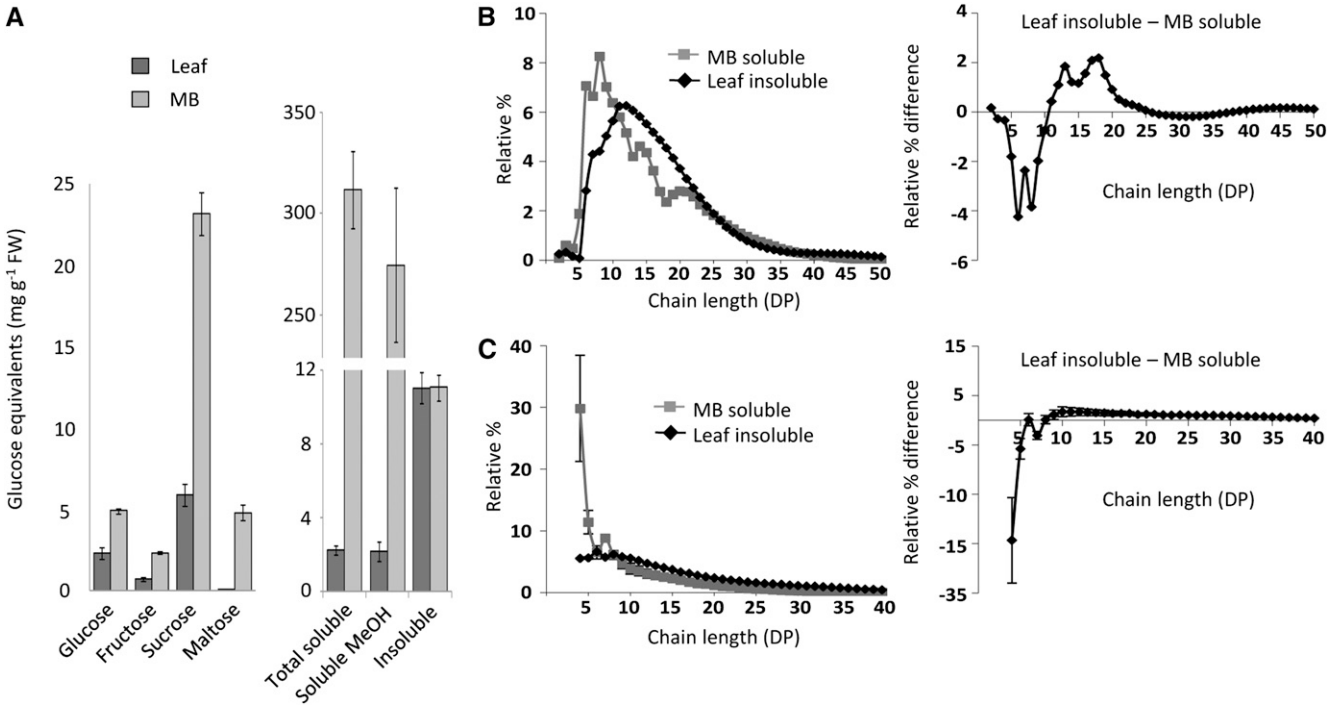

Figure 3. Carbohydrate Levels and Polyglucan Structural Analysis in *C. peltata* Tissues.

Sugars and polyglucans were extracted using perchloric acid from replicate samples of leaves and MBs harvested at the end of the day.

(A) Sugars (left panel) were analyzed using HPAEC-PAD. All sugars were significantly higher in MBs than in leaves (*t* test; P value ≤ 0.05). Soluble and insoluble polyglucans (right panel) were digested enzymatically and the released Glc determined spectrophotometrically. The proportion of soluble polyglucans that could be precipitated from the soluble fraction using methanol (MeOH-ppt; i.e., glycogen) was determined. Values are the mean ± SE (n = 4). Lower levels of insoluble glucan were detected in leaves harvested at the end of the night. FW, fresh weight.

(B) Methanol precipitated soluble MB polyglucans and insoluble leaf polyglucans were debranched and linear chains analyzed for their DP by HPAEC-PAD. CLDs are displayed as relative percentages of the total (left panel). Values are the mean ± SE (n = 4). When absent, error bars are smaller than the symbols. The relative percentage difference obtained by subtracting one data set from the other is shown on the right (errors from the two data sets are summed).

(C) Before debranching and HPAEC-PAD analysis (as shown in **[B]**), external chains of extracted polyglucans were first shortened by β-amylase treatment, providing information on the distance between branching points (for further explanation, see Supplemental Figure 2 online). External chains are reduced to a DP of 2 or 3. Only chains with a DP of 4 or greater are shown.

by RNA sequencing (RNA-seq). The broadest possible information about the *C. peltata* transcriptome was obtained by sequencing normalized leaf and MB cDNA libraries, obtained from extracted mRNA, using the GS FLX 454 platform (Roche Life Sciences). After quality control and adapter sequence removal, the resulting 997,683 reads were preassembled into 38,972 contigs using the GS De Novo Assembler software from 454 Roche Life Sciences (see Supplemental Figure 3 online). Next, we used Illumina sequencing of three replicate samples to generate quantitative transcript information for leaves and MBs. Sequencing using a Genome Analyzer GAIIx resulted in ~60 million 76-bp reads that were assembled into contigs using Velvet and Oases (Zerbino and Birney, 2008) (www.ebi.ac.uk/~zerbino/oases) by incorporating sequence information from the preassembled contigs from the 454 sequencing. This resulted in a transcript assembly containing a total length of 4,549,006 bp in

Figure 2. (continued).

(C) Transmission electron micrograph of leaf section displaying epidermal cell and palisade mesophyll cell chloroplasts with thylakoids and starch granules. Starch granules were present in chloroplasts of all different cell types of *C. peltata* leaves examined. No deposition of large amounts of soluble polysaccharides could be detected.

(D) Light microscopy of transverse section of MB showing the epidermal cell layer (epi) surrounding uniform parenchymal cells (par).

(E) Transmission electron micrograph of MB sections displaying densely packed parenchymal cells containing spherical glycogen-filled plastids (GP) and lipid droplets (LD).

(F) and **(G)** Transmission electron microscopy magnifications of a MBs plastid surrounded by a double membrane (black arrows). Small internal membrane systems were visible (**[G]**, white arrow), but most of the volume is occupied by 20- to 30-nm glycogen particles.

5992 contigs. The contigs average length was 758 bp, with an N50 of 990 bp (i.e., all contigs of 990 bp contain at half of the total of the total sequence length). Contigs derived from the 454 sequencing to which too few Illumina reads matched for them to be included in the transcript assembly were retrieved using MUMmer software (Kurtz et al., 2004). A detailed procedure of the sequencing experiments and database assemblies is available in Supplemental Methods 1 online, and all raw data have been submitted to ArrayExpress (www.ebi.ac.uk/arrayexpress).

To assign expression levels to the different contigs in the transcript assembly (hereafter referred to as transcripts), Illumina reads from each sample were individually mapped onto the transcripts using the CLC Genomics Workbench (CLC Bio). In total, 73.6% of the Illumina reads could be mapped. The distribution of read counts versus transcript frequency was comparable between the biological replicates and the two tissues (see Supplemental Figure 4 online). The correlations between samples from the same tissue were much stronger than between the different tissues (see Supplemental Figure 5 online). Finally, as the retrieved read counts differed slightly for each sample (see Supplemental Figures 4 and 5 online), we applied library size normalization (Mortazavi et al., 2008; Robinson and Oshlack, 2010).

As no reference genome is available for *C. peltata*, transcripts were annotated de novo using BLAST2Go (Götz et al., 2008; see Supplemental Methods online), using the *Arabidopsis* TAIR9 database. Of the 5992 transcripts, 5043 (82%) could be annotated (see Supplemental Data Set 1 online). In some cases, more than one *C. peltata* transcript matched the same *Arabidopsis* BLAST hit. This could result from nonoverlapping sequence fragments from the same mRNAs, resulting in two or more transcripts during transcriptome assembly. Alternatively, the existence of additional homologs in the *C. peltata* genome might also account for this observation. Furthermore, as suggested by Oases during transcriptome assembly, differential splicing occurred in up to 2.4% of all transcripts. However, we verified that differential splicing did not occur in the genes involved in storage carbohydrate and Suc metabolism (see below).

Key Carbohydrate Metabolic Genes Are Differentially Regulated to Achieve Starch or Glycogen Synthesis in Leaves and MBs

Transcripts differentially expressed between leaf and MB samples were identified using the R Bioconductor package edgeR (Robinson et al., 2010). Stringent criteria for differentially expressed transcripts were applied: a $\log_2$(fold change) smaller than -2 or larger than 2, a P value < 0.001, and at least 30 read counts (combined from all samples). Of the annotated transcripts, 1873 (37%) met these criteria (Figure 4A), 759 of which were more highly expressed in MBs, and 954 more highly expressed in leaves (Figure 4B). Also, 24 transcripts were uniquely expressed in MBs and 136 uniquely in leaves (in some cases with fewer than 30 transcripts). To gain insight into the metabolic processes over- and underrepresented at the transcriptional level in leaves or MBs, we categorized all 5043 transcripts according to their metabolic function based on MapMan software (see Supplemental Figure 6 online; Usadel et al., 2009; http://mapman.mpimp-golm.mpg.de/). A significant overrepresentation (compared with all transcripts) in the categories *minor carbohydrate metabolism*, *fermentation*, *cell wall*, *lipid metabolism*, *hormone metabolism*, and *miscellaneous* and *signaling* and an underrepresentation in the categories *photosynthesis*, *mitochondrial electron transport/ATP synthesis* and *protein* (Figure 4C, asterisk) was found for the transcripts in MBs. In leaves, *photosynthesis*, *major carbohydrate metabolism*, *secondary metabolism*, *tetrapyrrole synthesis*, *redox*, and *misc* were significantly overrepresented and *mitochondrial electron transport/ATP synthesis*, *cell wall*, *RNA*, *protein*, and *cell* were underrepresented (Figure 4C).

To understand the differential programming of the biosynthetic machinery required to produce either MB glycogen or leaf starch, we searched for transcripts of genes involved in central carbon metabolism and in the metabolism of Suc. We also searched for transcripts of genes homologous to those from *Arabidopsis* with known functions in starch synthesis and degradation (Table 1). Expression of plastidial phosphoglucose isomerase (*PGI1*), which catalyzes the interconversion of Fru-6-phosphate and Glc-6-phosphate, was higher in leaves, presumably reflecting the fact that the Calvin cycle provides substrates for starch biosynthesis in leaves (Streb et al., 2009). Transcripts encoding the triose-phosphate/phosphate translocator, involved in the export of photosynthates from chloroplasts, were also abundant in leaves. By contrast, *PGI1* expression was lower in MBs and the expression of the triose-phosphate/phosphate translocator was undetectable. However, expression of the structurally related plastid envelope transporter, GPT2, was higher in MBs than in leaves (Table 1). GPT2 mediates import of Glc-6-phosphate from the cytosol and presumably supplies the substrates for glycogen synthesis in MB plastids.

Consistent with the heterotrophic metabolism of MBs, we observed a significant higher transcript levels for SUS4 (the Suc synthase isoform most abundant and ubiquitously expressed in *Arabidopsis* tissues) and for two neutral invertases in MBs, suggesting that both mechanisms for Suc catabolism are active in MBs to fuel glycogen and lipid synthesis. Transcript levels of the cytosolic phosphoglucose isomerase (PGI2), the cytosolic UDP-glucose pyrophosphorylase (UGP2), and the cytosolic phosphoglucomutase (PGM3), all of which are needed for both autotrophic and heterotrophic metabolism, were similar in MBs and leaves.

There were marked differences in the expression of genes encoding subunits of ADPglucose pyrophosphorylase, the hetero-tetrameric enzyme downstream of PGI that synthesizes the ADP-glucose substrate for glucan synthesis. The regulatory large subunit gene *APL1* (for ADPglucose pyrophosphorylase large subunit 1) was expressed in leaves but not MBs (Table 1). By contrast, the large subunit gene *APL3* was highly upregulated in MBs. These data are in agreement with previous findings in other species that the large subunits are differentially expressed in photosynthetic and heterotrophic tissues and consistent with the idea that the enzymes in these tissues may be differently regulated (Crevillén et al., 2005). Interestingly, two transcripts homologous to the small, catalytic subunit were detected in both tissues but appeared to be inversely regulated, suggesting that there may be two *APS1*-like (for ADP-glucose pyrophosphorylase small subunit 1) genes in *C. peltata*.

Transcripts for all known SSs were detected in leaves, reflecting the fact that production of complex starch granules requires the combined actions of these enzyme isoforms. However, striking differences were observed in the isoform-specific expression

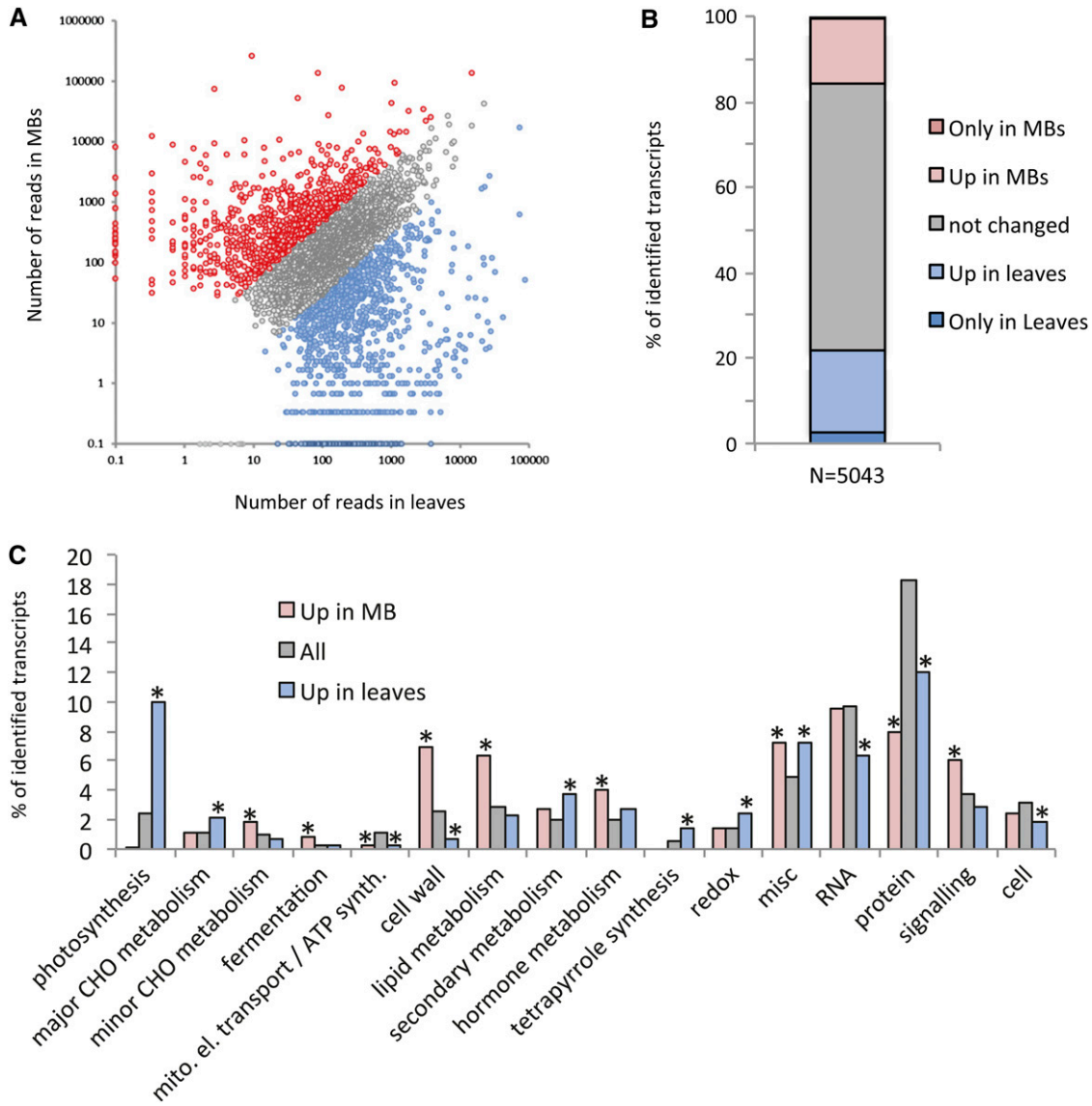

Figure 4. Quantitative Gene Expression in *C. peltata* Leaves and MBs.

Non-normalized cDNA, obtained from leaf and MBs RNA, was sequenced using the Illumina Genome Analyzer GAIIx. Triplicate samples were analyzed. **(A)** Assembled contigs were annotated using Blast2Go (www.blast2go.org) using the *Arabidopsis* TAIR9 database. An e-value threshold of 10^{-5} was used, resulting in 5043 transcripts (see Supplemental Data Set 1 online). Mean read counts for each transcript in each tissue are plotted. Colored points represent significantly upregulated or uniquely expressed genes in leaves (blue) and in MBs (red).

(B) A total of 136 transcripts were only expressed in leaves and 24 only in MBs. *t* test (P value < 0.001) and a $\log_2$(fold change) of the mean number of reads throughout the biological triplicates revealed 954 transcripts upregulated significantly in leaves and 759 upregulated significantly in MBs.

(C) Metabolic annotation was assigned to each transcript using MapMan (mapman.mpimp-golm.mpg.de). Categories indicated with an asterisk were significantly over- or underrepresented, relative to all the transcripts, showing P values < 0.05 in Fisher's exact test. CHO, carbohydrate; el., electron; mito, mitochondrion.

levels in MBs. *GBSS*, *SSIII*, and *SSIV* expression were all much lower in MBs than in leaves, whereas *SSI* expression was much higher (Table 1). *SSII* transcripts were detected in both MBs and leaves. Thus, differences in the relative abundance of SS isoforms in MBs and leaves likely contributes to the accumulation of soluble glycogen (which is rich in short chains) and of insoluble starch (which has a greater proportion of longer chains) in these tissues, respectively. Our data are consistent with the proposed role for SSI in the production of short chains of amylopectin, while SSII and SSIII preferentially produce intermediate and long glucan chains, respectively (Tomlinson and Denyer, 2003; Zhang et al., 2008; Szydlowski et al., 2009). GBSS synthesizes the linear amylose fraction of starch. Amylose is readily detectable as it stains intensely with iodine, but none was detected in MBs, consistent with the greatly reduced *GBSS* expression. The role of SSIV is less clear than for other SS isoforms, but it has been implicated

Table 1. Differences in Transcript and Protein Abundances for Genes Involved in Starch and Suc Metabolism in *C. peltata*

			Sequencing				Proteomics			
AGI Code[a]	Name	Description	Reads Leaf[b]	Reads MBs[b]	Log_2 (FC)[c]	P Value	nSpC Leaves	nSpC MBs	FC	P Value
Starch synthesis										
AT5G51820	*PGM1*	*PHOSPHOGLUCOMUTASE1*	1,627	2,193	0.11	7.36E-01	0.22	0.34	1.56	1.41E-01
AT4G24620	*PGI1*	*PHOSPHOGLUCOSE ISOMERASE1*	584	222	−1.79	2.28E-07	0.40	0.05	−7.52*	1.17E-04
AT5G19220	*APL1*	*ADP-Glc PYROPHOSPHORYLASE*	595	–	Leaf only	1.33E-42	1.26	0.23	−5.38*	3.08E-03
		LARGE SUBUNIT1	595	1	−9.61*	3.65E-43	0.76	0.26	−2.93	7.61E-02
AT4G39210	*APL3*	*ADP-Glc PYROPHOSPHORYLASE LARGE SUBUNIT3*	263	27,653	6.41*	1.29E-56	–	1.53	MB only	6.79E-02
AT5G48300	*APS1*	*ADP-Glc PYROPHOSPHORYLASE*	4,325	16,178	1.58	1.04E-06	1.79	2.80	1.57	2.06E-01
		SMALL SUBUNIT1	459	149	−2.05*	5.26E-09	–	–	–	–
AT1G32900	*GBSS*	*GRANULE BOUND STARCH SYNTHASE*	787	37	−4.67*	3.62E-29	–	–	–	–
			461	31	−4.34*	2.41E-25	–	–	–	
			430	24	−4.43*	6.19E-24	–	–	–	–
AT5G24300	*SSI*	*STARCH SYNTHASE I*	58	8,872	6.91*	1.84E-58	0.08	1.53	18.87*	6.39E-03
AT3G01180	*SSII*	*STARCH SYNTHASE II*	353	138	−1.65	3.50E-06	–	–	–	–
AT1G11720	*SSIII*	*STARCH SYNTHASE III*	1,456	109	−4.02*	1.81E-26	–	–	–	–
AT4G18240	*SSIV*	*STARCH SYNTHASE IV*	460	118	−2.33*	1.12E-10	–	–	–	–
AT2G36390	*SBE3*	*STARCH BRANCHING ENZYME3*	117	167	−0.22	5.20E-01	–	–	–	–
AT5G03650	*SBE2*	*STARCH BRANCHING ENZYME2*	1,939	2,108	−0.95	4.93E-02	0.34	1.55	4.57*	1.63E-02
			88	65	0.23	1.49E-02	–	–	–	–
AT2G39930	*ISA1*	*ISOAMYLASE1*	251	47	−2.73*	6.39E-12	–	–	–	–
Starch degradation										
AT1G10760	*GWD1*	*GLUCAN WATER DIKINASE1*	141	47	−1.79	2.07E-05	–	–	–	–
			795	402	−1.26	1.51E-04	–	–	–	–
AT3G52180	*SEX4*	*PHOSPHO-GLUCAN PHOSPHATASE*	1,273	1,005	−0.69	3.32E-02	–	–	–	–
AT3G01510	*LSF1*	*LIKE SEX FOUR1*	221	15	−4.30*	5.30E-20	–	–	–	–
AT3G23920	*BAM1*	*β-AMYLASE1*	1,064	367	−1.88	2.58E-08	–	–	–	–
AT4G17090	*BAM3*	*β-AMYLASE3*	6,256	157	−5.71*	3.98E-47	–	–	–	–
AT4G09020	*ISA3*	*ISOAMYLASE3*	269	2,318	2.77*	1.74E-15	0.03	0.56	22.22*	1.68E-02
AT5G04360	*LDA1*	*LIMIT DEXTRINASE1*	359	308	−0.54	1.10E-01	–	–	–	–
AT5G64860	*DPE1*	*DISPROPORTIONATING ENZYME1*	232	518	0.88	9.53E-03	–	–	–	–
Suc metabolism										
AT4G02280	*SUS3*	*SUCROSE SYNTHASE3*	197	132	−0.97	6.14E-03	–	–	–	–
			154	131	−0.61	9.79E-02	–	–	–	–
AT3G43190	*SUS4*	*SUCROSE SYNTHASE4*	1,045	9,941	2.89*	2.76E-17	2.07	4.87	2.35*	1.31E-02
AT5G42740	*PGIC*	*CYTOSOLIC PHOSPHOGLUCOSE ISOMERASE*	318	390	0.03	9.24E-01	0.42	0.49	1.16	5.47E-01
AT5G17310	*UGP2*	*UDP-Glc PYROPHOSPHORYLASE2*	1,269	2,381	0.56	7.94E-01	1.42	1.77	1.25	5.58E-01
AT1G23190	*PGM3*	*CYTOSOLIC PHOSPHOGLUCOMUTASE3*	94	88	−0.91	1.29E-02	1.16	1.44	1.24	6.02E-02
			104	151	−0.03	8.75E-01	–	–	–	–
AT3G59480	*FCK*	Carbohydrate Kinase Family Protein	679	2,539	1.53	3.39E-06	1.87	2.28	1.22	2.12E-01
AT4G29130	*HXK1*	*HEXOKINASE1*	805	668	−0.63	5.48E-02	–	–	–	–
			693	439	−1.07	1.27E-03	–	–	–	–
AT3G06500	*INVC*	*ALKALINE/NEUTRAL INVERTASE C*	663	7,661	3.23*	1.58E-20	–	–	–	–
AT4G09510	*INV2*	*CYTOSOLIC NEUTRAL INVERTASE2*	213	1,115	2.05*	2.81E-09	–	0.16	MB only	5.45E-02
AT1G61800	*GPT2*	*Glc-6-PHOSPHATE TRANSPORTER*	123	2,306	3.96*	3.66E-26	–	–	–	–
AT5F16150	*GLT1*	*Glc TRANSLOCATOR1*	375	410	−0.13	7.25E-01	–	–	–	–
			166	173	−0.4	2.50E-01	–	–	–	–
AT5G46110	*TPT1*	*TRIOSE-PHOSPHATE TRANSLOCATOR1*	539	–	Leaf only	4.41E-50	1.67	0.00	Leaf only	2.62E-04
			1,013	–	Leaf only	4.62E-61	0.81	0.00	Leaf only	2.15E-03
			10	–	Leaf only	1.77E-04	–	–	–	–
			1,761	–	Leaf only	5.43E-61	–	–	–	–

Sequence contigs (transcripts) were annotated against the *Arabidopsis* TAIR9 database. Proteins abundance is given as normalized spectral counts identified by mapping the peptides onto the transcript databases. Significant differences in transcript and/or protein abundances are marked with an asterisk. AGI, Arabidopsis Genome Initiative. Dashes indicate where transcripts or peptides were not detected, or p-value not calculated.

[a]More than one transcript can be assigned to the same gene when each contig maps to a different part of the transcript or if *C. peltata* possesses duplicate genes.

[b]Total reads from the replicate samples are given for each transcript.

[c]The fold change (FC) was calculated after correction for the total reads from each sample and cannot be directly calculated total reads.

in starch granule initiation. *Arabidopsis ssiv* mutants have fewer, abnormally shaped granules in their chloroplasts than the wild type (Roldán et al., 2007). In this view, the observed reduction in *SSIV* expression in MBs is consistent with the absence of starch granules but suggests an alternative mechanism for glycogen initiation.

Concurrently with chain elongation by SSs, the glucan branching pattern is determined by the combined actions of BEs and DBEs (Tomlinson and Denyer, 2003). We did not observe changes in the expression of either *BE2* or *BE3*. Of the DBEs, *ISA1* expression was decreased in MBs, while *ISA3* expression was increased (Table 1). ISA1 is most active on glucan substrates with long external chains (Hussain et al., 2003; Delatte et al., 2005; Wattebled et al., 2005) and has a major role in promoting the crystallization of amylopectin. By contrast, ISA3 is involved in the removal of short amylopectin chains and has been associated with the process of starch degradation (Wattebled et al., 2005; Delatte et al., 2006). The expression of genes encoding other enzymes associated with starch breakdown, including glucan water dikinase (GWD1; Yu et al., 2001), the phosphoglucan phosphatase STARCH-EXCESS4 (SEX4; Zeeman et al., 1998; Kötting et al., 2009), and its homolog LIKE SEX FOUR1 (LSF1; Comparot-Moss et al., 2010), the β-amylases BAM1 and BAM3 (Fulton et al., 2008), and DISPROPORTIONATING ENZYME1 (DPE1; Critchley et al., 2001) were either unchanged in expression or lower in MBs compared with leaves (Table 1).

The system-wide view obtained by RNA-seq illustrates not only the major differences in metabolism associated with the autotrophic versus heterotrophic growth but also that key components involved in starch metabolism are differentially balanced between leaves and MBs to allow the synthesis of the two types of polyglucan. Importantly, these data show that not just one, but rather a combination of many genes, is differentially regulated to achieve either starch or glycogen synthesis.

Quantitative Shotgun Proteomics Confirms Differential Metabolic Programming Observed in MBs by RNA-Seq

Transcript levels do not necessarily correlate with protein abundances (Baerenfaller et al., 2012). Therefore, to determine if the results obtained from the transcript sequencing were reflected at the protein level, we performed large-scale proteome profiling of leaves and MBs using label-free quantitative mass spectrometry (MS). Proteins from leaves and from MBs were extracted in three independent biological replicates, separated by SDS-PAGE (see Supplemental Figure 7A online), in-gel digested by trypsin, and subjected to tandem MS. Database searching against the Velvet/Oases assembly resulted in the identification of 1714 proteins with at least two unique peptides. A total of 1512 and 1359 were identified in leaves and MBs, respectively (Figures 5A and 5B; see Supplemental Figure 7B online). Methods and criteria used for MS, protein identification, and quantification are detailed in Supplemental Methods 1 online. The proteomics data were exported to the PRIDE database (Wang et al., 2012). There were 355 proteins found only in leaves and 202 only in MBs, of which 154 and 26, respectively, were sufficiently abundant and reliably detected as to be defined as unique to these tissues. The number of proteins identified in each replicate of leaves and of MBs was similar, and overlap between the replicates was high, indicating a good experimental reproducibility (see Supplemental Figures 7C and 7D online). Also, Pearson correlation factors were high between the replicates and decreased when leaves were compared with MBs (see Supplemental Figure 7E online). Quantitative information was obtained for all identified proteins using normalized spectral counting (nSpC) (Baerenfaller et al., 2008; Bischof et al., 2011) (see Supplemental Figure 8 online) to define proteins that were significantly more abundant in leaves or in MBs. These proteins have a minimum twofold change in abundance (mean nSpC), a P value < 0.05, and have been identified with at least 10 peptides throughout all replicates. In total, 109 proteins were significantly more abundant in leaves, and 158 were more abundant in MBs (Figure 5B).

Functional analysis of all identified proteins (see Supplemental Figure 9A online) further highlights the autotrophic metabolism in leaves, as proteins belonging to *photosynthesis* are strongly overrepresented in leaves and underrepresented in MBs (see Supplemental Figure 9B online). Furthermore, similar to the transcriptome analysis, proteins involved in *fermentation* and *lipid metabolism* were overrepresented in MBs (see Supplemental Figure 9B online), consistent with their heterotrophic metabolism and observed function in the storage of lipids (Figure 2).

In most cases, differences in protein abundances between leaves and MBs were consistent with the differences in transcript abundances (Figure 5C; see Supplemental Data Set 2 online). We observed a concomitant down- and upregulation in 60% of the 447 protein transcript pairs in which the protein level changed significantly (Figure 5D). Only seven proteins showed significant opposite fold changes between protein and transcript levels (Figures 5C and 5D; see Supplemental Data Sets 1 and 2 online). Of the 1267 genes that were not significantly changed at the protein level (Figures 5A and 5B), only 13 and 17% were significantly upregulated at transcript level in MBs and leaves respectively (Figure 5D), with the remaining 70% unchanged. Together, these data suggest that the transcriptome is more dynamic than the proteome and that ~30% of the proteome is regulated by both transcriptional and posttranslational mechanisms, which is in line with a recent integrated genome- and proteome-wide study in *Arabidopsis* (Baerenfaller et al., 2012).

Proteins were detected for 15 of the genes listed in Table 1, most of which had correlated protein and transcripts levels between leaves and MBs. PGI1, APL1, and TPT1 were significantly more abundant in leaves compared with MBs, whereas SUS4, SSI, and ISA3 were significantly more abundant in MBs (Table 1). Interestingly, a major increase in BE2 protein abundance was detected despite unaltered transcript levels, suggesting that branching activity is elevated in MBs. Because branching is one of the key steps determining polyglucan structure, we confirmed increased BE activity in MBs using activity assays (Figure 4E). Soluble proteins from leaves and MBs were separated by native PAGE, and BE activity was assessed after incubation in Glc-1-phosphate, AMP, and phosphorylase *a*. Activity bands of four assays, each performed with different protein amounts, were quantified by densitometry (Figure 4E), showing that BE activity was ~4 times higher in MBs than in leaves, confirming the proteomics data.

Collectively, the RNA-seq and quantitative proteome data indicate that there are major differences in the abundances of

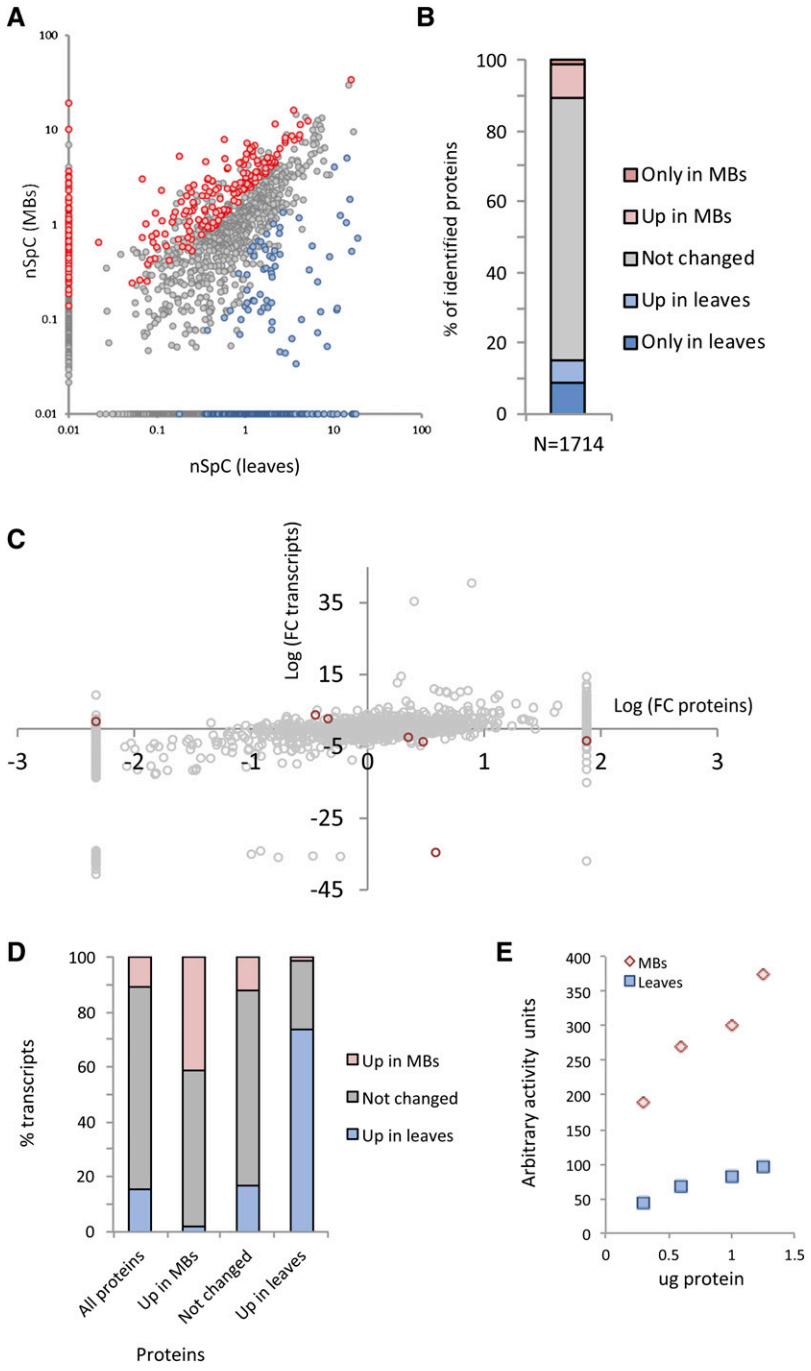

Figure 5. Quantitative Protein Accumulation in *C. peltata* Leaves and MBs Determined by Tandem MS.

Triplicate extracts of proteins were separated by SDS-PAGE and in-gel digested using trypsin, and the resulting peptides were analyzed using an Orbitrap mass spectrometer.

(A) In total, 1714 proteins were identified. Quantitative information was obtained for all identified proteins using normalized spectral counting (nSpC). Identified proteins were visualized by plotting the respective number of nSpC. Significantly more abundant proteins in leaves and in MBs were represented in blue and red, respectively. To display proteins identified only in MBs or only in leaves, the smallest nSpC value of the respective data set was arbitrarily given. There were 355 proteins found only in leaves and 202 only in MBs, of which 154 and 26, respectively, were sufficiently abundant and reliably detected as to be defined as unique to these tissues.

(B) *t* test (P value < 0.05) and a twofold change of the mean number of nSpC revealed 109 proteins significantly more abundant in leaves and 158 significantly more abundant in MBs in addition to those only found in one or the other tissue.

specific isoforms of all three enzyme classes involved in glucan biosynthesis, SSs, BE, and DBEs, which can explain glycogen accumulation in MBs and starch accumulation in leaves.

DISCUSSION

Using a broad palette of targeted and high-throughput methods allowed us to characterize the two storage polyglucan types found in the tropical tree *C. peltata* and dissect the reprogramming of the carbohydrate biosynthetic machinery. There is an enormous difference in the extent of polyglucan synthesis between leaves and MBs. Glycogen levels in MBs are extremely high, accounting for a third of the fresh weight of the tissue. Therefore, the metabolism of *C. peltata* MBs can be viewed as a natural model system that generates huge amounts of readily metabolizable soluble polyglucans.

We observed high levels of small sugars, primarily Suc imported from source tissues, but also maltose and other small malto-oligosaccharides, in MBs. In leaves, maltose is the major starch breakdown product, generated by β-amylases and exported from chloroplasts via the inner envelope maltose transporter MEX1 to fuel metabolism at night (Niittylä et al., 2004; Zeeman et al., 2010; Ball et al., 2011). The presence of maltose and malto-oligosaccharides in MBs could be explained by concurrent degradation accompanying glycogen synthesis. Such turnover has been observed in *Arabidopsis* mutants lacking ISA1 and/or ISA2 (Delatte et al., 2005), which make phytoglycogen rather than starch. MBs express a number of enzymes known to be involved in starch degradation, and, although β-amylase expression was lower than in leaves, maltose might accumulate if the MEX1 transporter is not present (unfortunately, transcripts corresponding to MEX1 were not detected, making this idea hard to evaluate). However, it is questionable whether the glycogen in the MBs is remobilized by the plant, as the MB represents a terminal tissue type that will senesce if not consumed. It cannot be ruled out that maltose and malto-oligosaccharides might be generated de novo, and they may function as glycogen priming units, although such a role is highly speculative.

Structural analyses of MB glycogen and leaf amylopectin revealed typical differences in polyglucan architecture. Glycogen was enriched in short chains and had branch points very close to one another compared with amylopectin. These qualities likely prevent the formation of secondary structures within the polyglucan and render this polymer type soluble. Solubility and granule/particle size are two important variables that are important in the improvement of starch crops. Structural changes leading to enhanced solubility will influence cooking properties (e.g., gelatinization temperature) and starch digestibility and may affect processing costs in the starch industry and the bioenergy sector.

Our use of 454 and Illumina sequencing to generate quantitative transcriptional maps of *C. peltata* provides critical insight into the differences in gene expression that underlie its ability to synthesize two polyglucan types in a tissue-dependent way (Figure 6). Combining this with proteome profiling confirmed that many of the observed changes in gene expression were reflected at the protein and presumably enzyme activity levels. Very few proteins were identified that showed opposite changes in proteins and transcript levels. However, our data also suggest that, in some cases, posttranscriptional regulation of the proteome occurs (i.e., BE2). The profiling approaches yielded expected results in terms of illustrating the autotrophic metabolism of leaves (e.g., the expression of photosynthetic genes) and the heterotrophic metabolism of MBs (e.g., expressing genes required for Suc catabolism of and hexose phosphate uptake into plastids). More importantly, however, they gave specific information about the nonobvious changes associated with the flux into glucan biosynthesis and the factors controlling its structure and form (Figure 6).

The expression of AGPase, the enzyme controlling the flux into glucan biosynthesis, was much higher in MBs, and the subunit composition was different from that in leaves. This probably reflects both a higher capacity for ADPglucose production, needed to support high rates of glycogen synthesis, and altered regulation of the enzyme, such that flux through the pathway depends on different factors in the two tissues. In leaves, flux into starch biosynthesis is carefully controlled and coordinated with Suc production (Geigenberger, 2011). This serves to partition photoassimilates optimally between immediate plant growth and short-term storage for subsequent use at night when photosynthesis stops. By contrast, in a terminal storage tissue like an MB, flux into glycogen biosynthesis will need to be coordinated with other plastidial pathways like fatty acid biosynthesis, presumably entailing different mechanisms of enzyme regulation.

In MBs, there were many changes in the expression of genes encoding the starch metabolic enzymes compared with leaves (Figure 6). In leaves, moderate transcript levels were detected for five distinct SSs, with highest levels observed for SSIII and GBSS, while SSI expression was lowest. This reinforces the idea that all five SSs have distinct roles in the biosynthesis of the starch granule (Zeeman et al., 2010). The situation is very different for MBs, where SSI is by far the dominant isoform, being more than 100-fold upregulated at the transcript level and almost 20-fold higher at the protein level compared with leaves. The other SS isoforms had transcript levels up to 20-fold lower in MBs than in leaves. Previous studies suggested that SSI may preferentially generate short chains in amylopectin (Tomlinson

Figure 5. (continued).

(C) Transcript-protein pairs were visualized by plotting the $\log_2$(fold changes) [FC] of the mean reads number and the mean nSpCs. Very few genes (in red) displayed a significantly opposite trend in transcript and protein levels (see Supplemental Data Set 2 online).

(D) Significant up- and downregulation is shown for the transcripts corresponding to all identified proteins, for proteins significantly more abundant in MBs (Up in MBs), for proteins whose abundance was not changed, and for proteins significantly more abundant in leaves (Up in leaves).

(E) In-gel assay for BE activity in leaves and MBs. Soluble proteins were separated by native PAGE, and branching activity was tested by incubation in Glc-1-P, AMP, and phosphorylase *a*. Activity bands of four independent assays were quantified and displayed according to the respective micrograms of protein loaded.

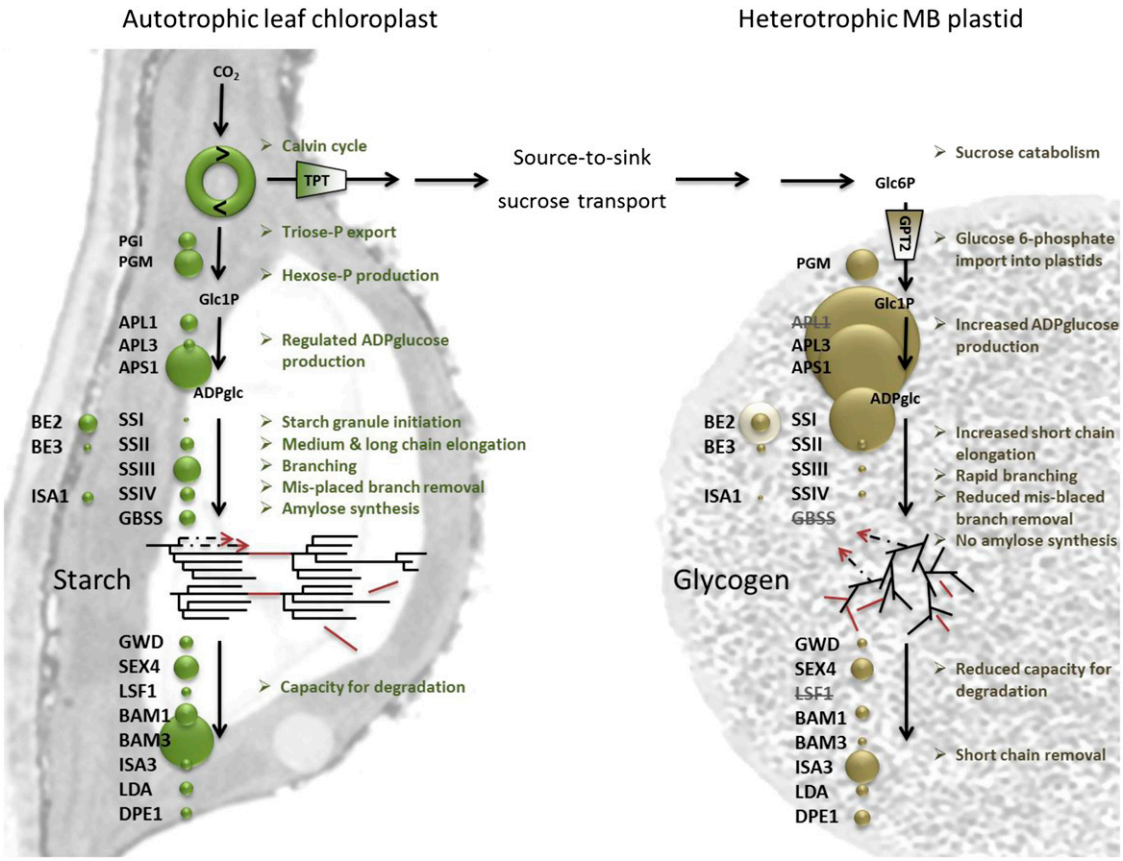

Figure 6. A Model Depicting the Major Changes in Expression in Genes Involved in the Production of Starch in Leaves and Glycogen in MBs.

The areas of the circles adjacent to genes reflect the expression levels, based on the total read count presented in Table 1. Genes with a very low read count in MBs are in gray and crossed out. Note the larger circle for BE2 in MBs, reflecting the increased protein abundance despite unchanged transcript levels.

and Denyer, 2003; Zhang et al., 2008; Szydlowski et al., 2009), as *ss1* mutant amylopectin is deficient in short chains and richer in intermediate- and long-chain fractions (which are synthesized by SSII and SSIII). The massive upregulation in MBs of SSI and downregulation of other SS isoforms greatly polarizes the balance of chain elongating reactions in favor of short-chain biosynthesis, simultaneously explaining one of the key features of glycogen and the absence of detectable amylose in MBs (the latter due to the decrease in GBSS expression). Interestingly, no change in transcription was detected for either BE2 or BE3 genes. However, protein quantification revealed more than a fourfold increase in BE2 protein, and in-gel assays revealed a substantial increase in BE activity, consistent with the idea that BE2 protein abundance is regulated posttranscriptionally.

In other plants (including the cereals maize [*Zea mays*], rice [*Oryza sativa*], and barley [*Hordeum vulgare*] as well as *Chlamydomonas reinhardtii* and *Arabidopsis*), mutation of the ISA1-type DBE results in the production of water-soluble polysaccharides, predominantly a glycogen-like polymer, phytoglycogen. Phytoglycogen is synthesized either in place of starch or alongside starch that, in some cases, was reported to contain aberrant amylopectin (Zeeman et al., 2010 and references therein). In MBs, ISA1 transcripts were fivefold lower than in leaves. This downregulation is consistent with its proposed function in helping to tailor or trim amylopectin during starch biosynthesis (Ball et al., 1996), possibly by removing branch points that are too close together (Delatte et al., 2005; Streb et al., 2008). In this way, ISA1 is proposed to facilitate the formation of crystalline structures within the amylopectin molecule, and there is no evidence that ISA1 plays a role in starch degradation (Streb et al., 2012). In *Arabidopsis* and potato (*Solanum tuberosum*), ISA1 forms a stable complex with ISA2 (Hussain et al., 2003; Delatte et al., 2005; Wattebled et al., 2005), but neither ISA2 transcript nor protein was detected in our study. By contrast, ISA3 was markedly upregulated in MBs, both at the transcript and protein levels. The proposed role of ISA3 is different from that of ISA1. ISA3 prefers substrates with very short external branches (Wattebled et al., 2005; Delatte et al., 2006), such as those produced by β-amylases during starch degradation (i.e., β-limit dextrins; see Supplemental Figure 2 online). Its activity is much lower on substrates such as amylopectin and glycogen (20- and 50-fold lower, respectively; Hussain et al., 2003). The significance of ISA3 induction in MBs is unclear, as the transcription of most of the other enzymes of starch breakdown are either unchanged or, in the case of the plastidial β-amylases,

decreased. However, it is worth noting that, while rich in short chains of DP 5 to 9, the MB glycogen lacked shorter chains of DP 2 to 4. If such very short chains were produced during glycogen synthesis, they may be removed by ISA3.

Together, these large-scale data sets provide a system-wide view for the quantitative balancing of multiple enzymes to achieve the specific synthesis of two different storage polyglucans in the same organism. This combination of biosynthetic components represents an archetype for future work in model organisms such as *Arabidopsis* to dissect further the role of individual enzymes in relation to each other. It seems likely that the differential programming of glucan metabolism in the MBs is accompanied by other changes at the cellular level, such as the production of lipid bodies, the shrinkage of the central vacuole, and the proliferation of plastids. Our initial functional analysis revealed several metabolic pathways differentially regulated between leaves and MBs, but further mining of our transcriptome and proteome data sets might shed light into these processes. These resources might also aid in the investigation of *C. peltata* as a potential source of biomedicines for the treatment of rheumatism, malaria, and diabetes (Pérez-Guerrero et al., 2001; Andrade-Cetto and Heinrich, 2005; Uchoa et al., 2010) or facilitate molecular-ecological studies into the mechanisms of ant–plant communication.

The production of glycogen in MBs represents a remarkable adaptation of *C. peltata* to its mutualistic lifestyle with ants. Being soluble, glycogen is more readily digested by ants than starch. Thus, glycogen synthesis might represent a compromise between the large amounts that could be stored as starch and the low amounts that could be stored as simple sugars (e.g., Suc or hexose sugars). Considering also the abundant lipid droplets, MBs must represent a very rich source of nutrition, in a form that can be readily transported back to the ants' nest. Interestingly, *C. peltata* is not unique in its ability to make glycogen. A similar ability was reported for another myrmecophytic plant from Australia, *Ryparosa kurrangii* (Webber et al., 2007). *R. kurrangii* is a member of the *Achariaceae* and is only distantly related to *C. peltata* (a member of the *Urticaceae*). It will be fascinating to discover if the same mechanism for glycogen production is used by this species.

In summary, this study provides an overview of carbohydrate biosynthesis in a nonmodel species to uncover the molecular determinants of polyglucan structure. We identify four changes (increased substrate biosynthesis, altered expression of chain-elongating SSs, increased BE activity, and decreased expression of the DBEs) that enable the switch from making modest amounts of the relatively complex structure, starch, to much larger amounts of the simpler structure, glycogen. It should be noted that there may also be other as yet unidentified factors involved in the production of either of the polymers. This not only helps define the specific functions of enzyme isoforms but also paves the way for manipulating the balance between them in crop plants to enable the synthesis of tailor-made polyglucans.

METHODS

Plant Material

Cecropia peltata was grown in a greenhouse with a relative humidity of ~60 to 70% and a temperature between 20 and 25°C. All MB and leaf samples were collected at the end of the day in summer when MB production was highest. Approximately 30 to 40 MBs were produced per day, per trichilium, and the MB emergence rate was highest on sunny days, between noon and 6 PM (Folgarait et al., 1994). The tree was protected from ants present in the greenhouse. Newly emerging MBs were frozen in liquid N_2 after harvesting, and material from the same trichilium was pooled. Leaf material was sampled at the same time, from a fully emerged leaf with an active trichilium and was frozen immediately in liquid N_2. Biological replicates from three active trichilia and the corresponding leaves were harvested. All samples were ground in liquid N_2 using glass beads and a Mixer Mill (Retsch).

Transmission Electron Microscopy

Leaf samples were cut into rectangles (2 × 1 mm), and MBs were cut in half crosswise. Samples were fixed in 2% (v/v) glutaraldehyde in 0.1 M sodium cacodylate buffer, pH 7.4, for 16 h at 4°C. Fixed samples were washed five times with ice-cold 0.1 M sodium cacodylate buffer, pH 7.4, postfixed for 16 h in 1% (w/v) aqueous osmium tetroxide, 0.1 M sodium cacodylate buffer, pH 7.4, at 4°C, washed again three times in ice-cold 0.1 M sodium cacodylate buffer, pH 7.4, and washed once in water at 25°C. Samples were dehydrated in an increasing ethanol series (50, 60, 70, 80, and 98% [v/v]) at 4°C for 2 h and finally in 100% (v/v) ethanol at 4°C for 16 h. Dehydrated samples were embedded in epoxy resin (Spurr's; Agar Scientific). Increasing ratios of Spurr's resin with ethanol were used for embedding (25, 50, and 75% [v/v], each step 16 h at 25°C and 100% [v/v], 7 d at 25°C). Ultrathin sections were cut with a diamond knife, collected on copper grids, and stained with uranyl acetate (2% [w/v] in 50% [v/v] acetone), washed three times with water, and stained again in Reynold's lead citrate. Stained sections were washed three times with water and examined using a Phillips BioTwin CM100 or a FEI Morgagni 268 transmission electron microscope.

Quantification of Starch, Soluble Polyglucans, and Sugars

Starch and soluble polyglucans were extracted from frozen powder using ice-cold 0.7 M perchloric acid in cooled glass homogenizers. Starch was separated from soluble sugars by centrifugation for 5 min at 3000*g*, 4°C. Pellets, containing the starch fraction, were washed with water and then at least three times with ethanol until the pellets were white. Pellets were resuspended in 1 mL of water. The soluble perchloric acid fraction was neutralized by adding cold 2 M KOH, 0.4 M MES, and 0.4 M KCl until a pH of between 5 and 7 was reached. Precipitated potassium perchlorate was removed by centrifugation for 10 min at 4°C, 16,100*g*. Two hundred and fifty microliters of the insoluble fraction were boiled for 15 min, cooled to 20°C, and mixed with 250 μL 50 mM sodium acetate, pH 4.8, 12.6 units of amyloglucosidase (EC 3.2.1.3), and 10 units of α-amylase (EC 3.2.1.98). For soluble polyglucan quantification, 100 μL of the soluble fraction was mixed with 100 μL 50 mM sodium acetate, pH 4.8, and 5 μL enzyme mixture containing 6.3 units of amyloglucosidase and 5 units of α-amylase. Starch and soluble polyglucans were hydrolyzed to Glc at 37°C for 2 h. For Glc quantification, 25 μL of the digest was mixed in a 200 μL assay containing 25 mM HEPES, pH 7.5, 1 mM $MgCl_2$, 1 mM ATP, 1 mM NAD^+, and 1.4 units hexokinase (EC2.7.1.1). The initial OD (340 nm) was measured, and 1 unit of Glc-6-phosphate dehydrogenase (EC1.1.1.49) was added to start the reaction. The conversion of NAD^+ to NADH was monitored using a Discovery XS-R microtiter plate reader (BIO-TEK Instruments). Maltose, Suc, Glc, and Fru were determined using HPAEC-PAD. Samples of the neutralized soluble fraction (100 μL) were applied to sequential 1.5-mL columns of DOWEX50 and DOWEX1 (Sigma-Aldrich). Neutral compounds were eluted with water, lyophilized, and dissolved in 100 μL of water for HPAEC-PAD analysis. A detailed description of the HPAEC-PAD analysis is provided in Supplemental Methods 1 online.

CLD Analysis

Insoluble starch or water-soluble polyglucans samples, equivalent to 100 μg Glc, were diluted to a final volume of 470 μL. Samples were boiled for 15 min and cooled to 20°C, and 25 μL 50 mM sodium acetate, pH 3.5, and 10,000 units *Pseudomonas amyloderanosa* isoamylase (EC 3.2.1.41) and 1 unit *Klebsiella planticolla* pullulanase (EC 3.2.1.68) were added. Starch and soluble polyglucans were debranched at 37°C for 2 h, and insoluble material was removed by centrifugation (5 min, at 16,000*g*, 20°C). Reactions were stopped by heating the samples to 95°C for 10 min, and insoluble material was removed by centrifugation (10 min at 1000*g*). Charged compounds were removed from the uncharged glucan chains using sequential 1.5-mL columns of DOWEX50 and DOWEX1. The resins were washed with water until the pH of the water was between 6 and 7. Two hundred microliters of the debranched samples or soluble sugars was diluted to 1 mL with 800 μL water and loaded onto the resin-containing columns. Uncharged compounds were eluted with three washes of 1 mL water, lyophilized, dissolved in 120 μL water, and centrifuged for 10 min at 3000*g*. One hundred microliters were transferred to snap-cap vials for HPAEC-PAD as described previously (Streb et al., 2008; see Supplemental Methods online).

For β-CLD analysis, 100 μg Glc equivalents of starch or soluble polyglucans samples were diluted with water to a final volume between 100 and 500 μL, depending on the sample volume required for 100 μg Glc equivalents. Samples were heated for 10 min at 95°C. Two-fifths of the sample volume of 200 mM MES, pH 6.5, 3 mM DTT, and 100 units of barley (*Hordeum vulgare*) β-amylase (Megazyme) were added. The mixture was incubated at 37°C for 3 h to shorten external glucan chains, and the digestion was terminated by heating for 5 min at 95°C. The β-limit-dextrin was precipitated 16 h at −20°C in 75% (v/v) methanol and collected by centrifugation for 10 min at 3000*g*, 4°C. The pellet was washed twice with cold 75% (v/v) methanol and dissolved in 110 μL water. Centrifugation for 10 min at 3000*g*, 4°C, removed aggregated proteins. One hundred microliters of the supernatant was used for CLD digestion with isoamylase and pullulanase, as described above.

RNA-Seq of the *C. peltata* Transcriptome

A detailed procedure of the *C. peltata* transcriptome sequencing and of the database assemblies is available in Supplemental Methods 1 online. Briefly, mRNA was isolated from frozen, powdered leaf or MB tissue using the Spectrum Plant Total RNA Kit (Sigma-Aldrich) according to manufacturer's instructions. cDNA was prepared using the Mint cDNA Synthesis Kit (Evrogen) with modification of the poly(A) tails. Normalization of cDNA prior to 454 sequencing was done using the Trimmer cDNA Normalization Kit (Evrogen) according to manufacturer's instructions. The 454 sequencing libraries were prepared with the GS Titanium General Library Preparation Kit (Roche Life Sciences) using 5 μg of normalized cDNA according to the manufacturer's protocol. Sequencing reactions were performed on a Roche Life Sciences 454 Genome Sequencer FLX. Illumina sequencing was performed by Fasteris on the Illumina Genome Analyzer GAIIx.

Protein Extraction and MS

Total proteins were extracted according to Saravanan and Rose (2004). MB or leaf material was homogenized on ice using an all-glass homogenizer in 1% (w/v) polyvinylpolypyrrolidone, 0.7 M Suc, 0.1 M KCl, 0.5 M Tris-HCl, pH 7.5, 100 mM EDTA, 2% (v/v) β-mercaptoethanol, and 2× protease inhibitor cocktail (Roche). An equal volume of phenol, pH 8, was added, mixed, and then subjected to centrifugation (30 min, 4000*g*, 4°C). Proteins in the phenol phase were precipitated overnight at −20°C in 5 volumes of 0.1 M ammonium acetate in methanol. Precipitated proteins were collected by centrifugation (5 min, 4000*g*, 4°C) and washed in methanol and then in 80% (v/v) acetone. Air-dried precipitated proteins were dissolved in 4% (w/v) SDS, 40 mM Tris, pH 6.8, and 2× protease inhibitor cocktail (Roche). Protein concentration was determined using a BCA Protein Assay Kit (Thermo Scientific) before adding 40 mM DTT. Proteins were heated for 5 min at 95°C, and 100 μg MB and leaf proteins was then subjected to SDS-PAGE on 12% (w/v) polyacrylamide gels. Protein bands were visualized by Coomassie Brilliant Blue staining according to standard procedures. Sample preparation, MS analysis, database mining, and label-free protein quantification were performed according to Baerenfaller et al. (2008) and Bischof et al. (2011) and are described in detail in Supplemental Methods 1 online.

Native PAGE

Tissues were ground in all-glass homogenizers, and soluble proteins were extracted in 100 mM MOPS, pH 7.2, 5 mM DTT, 10% (v/v) glycerol, 1 mM EDTA, and 50 mg mL^{-1} polyvinylpolypyrrolidone. Cell debris was removed by centrifugation (10 min, 16,000*g*, 4°C). Protein concentrations were determined by Bradford assay (Bio-Rad). Proteins (20 μg) were analyzed by native PAGE as described previously (Zeeman et al., 1998). Gels contained 6% (w/v) polyacrylamide. To assay BE activity, gels were rinsed with 50 mM HEPES-NaOH, pH 7.5, 2 mM DTT, and 10% (v/v) glycerol and incubated in the same medium plus 50 mM Glc-1-P, 2.5 mM AMP, and 50 units rabbit muscle phosphorylase *a*.

Accession Numbers

All raw sequence data have been submitted to ArrayExpress (www.ebi.ac.uk/arrayexpress) and are accessible with the code E-MTAB-1280. The proteomics data have been submitted to the PRIDE database (http://www.ebi.ac.uk/pride/) with accession numbers from 24090 to 24095.

Supplemental Data

The following materials are available in the online version of this article.

Supplemental Figure 1. Chain Length Distribution Measurements of Soluble and Insoluble Polyglucans.

Supplemental Figure 2. Interpretation of the β-Chain Length Distribution Analyses of Müllerian Body Glycogen and Leaf Starch.

Supplemental Figure 3. 454 Sequencing of Normalized *C. peltata* cDNA.

Supplemental Figure 4. Distribution of Read Counts per Transcript for Each Replicate Sample, Obtained from Illumina Sequencing.

Supplemental Figure 5. Correlation of Non-Normalized Transcript Read Counts between Tissues and between Biological Replicates.

Supplemental Figure 6. Metabolic Categorization of All Annotated Transcripts.

Supplemental Figure 7. Shotgun Proteome Analysis of *C. peltata* Leaves and Müllerian Bodies.

Supplemental Figure 8. Normal Distribution of the Log_2-Transformed Spectral Counts for Each Replicate Leaf and Müllerian Body Sample.

Supplemental Figure 9. Metabolic Categorization of All Identified Proteins

Supplemental Data Set 1. Transcript Profiling of Leaves and Müllerian Bodies.

Supplemental Data Set 2. Quantitative Proteome Profiling of Leaves and Müllerian Bodies.

Supplemental Methods 1. Methods for Carbohydrate Analysis, Transcript Profiling, and Quantitative Proteome Profiling.

ACKNOWLEDGMENTS

We thank the members of the Functional Genomics Center Zurich, Bernd Roschitzki, Paolo Nanni, Peter Gehrig, Claudia Fortes, Jonas Grossmann, Christian Panse, Simon Barkow-Oesterreicher, and Marzanna Küenzli, for their support in MS, bioinformatics, and sequencing. We also thank Matthias Hirsch-Hoffmann and Wilhelm Gruissem for their bioinformatics and scientific expertise as well as André Imboden, Andrea Gronau, and Christopher Ball for taking care of the *C. peltata* trees in the greenhouses. We acknowledge funding from ETH Zurich, the ETH Foundation (via a Heinz Imhof Fellowship to M.U., sponsored by Syngenta) and the Zurich-Basel Plant Science Centre (via a postdoctoral fellowship to S.B., funded by a donation from Syngenta). The funders had no role in study design, data collection and analysis, decision to publish, or preparation of the article.

AUTHOR CONTRIBUTIONS

S.B., M.U., S.S., and S.C.Z. conceived and designed the experiments. S.B., M.U., S.E., W.Q., and S.S. performed the experiments and analyzed the data. S.B. and S.C.Z. wrote the article.

Received January 22, 2013; revised March 15, 2013; accepted April 8, 2013; published April 30, 2013.

REFERENCES

Andrade-Cetto, A., and Heinrich, M. (2005). Mexican plants with hypoglycaemic effect used in the treatment of diabetes. J. Ethnopharmacol. **99:** 325–348.

Baerenfaller, K., Grossmann, J., Grobei, M.A., Hull, R., Hirsch-Hoffmann, M., Yalovsky, S., Zimmermann, P., Grossniklaus, U., Gruissem, W., and Baginsky, S. (2008). Genome-scale proteomics reveals *Arabidopsis thaliana* gene models and proteome dynamics. Science **320:** 938–941.

Baerenfaller, K., et al. (2012). Systems-based analysis of *Arabidopsis* leaf growth reveals adaptation to water deficit. Mol. Syst. Biol. **8:** 606.

Ball, S., Colleoni, C., Cenci, U., Raj, J.N., and Tirtiaux, C. (2011). The evolution of glycogen and starch metabolism in eukaryotes gives molecular clues to understand the establishment of plastid endosymbiosis. J. Exp. Bot. **62:** 1775–1801.

Ball, S., Guan, H.P., James, M., Myers, A., Keeling, P., Mouille, G., Buléon, A., Colonna, P., and Preiss, J. (1996). From glycogen to amylopectin: A model for the biogenesis of the plant starch granule. Cell **86:** 349–352.

Ball, S.G., and Morell, M.K. (2003). From bacterial glycogen to starch: Understanding the biogenesis of the plant starch granule. Annu. Rev. Plant Biol. **54:** 207–233.

Bischof, S., Baerenfaller, K., Wildhaber, T., Troesch, R., Vidi, P.A., Roschitzki, B., Hirsch-Hoffmann, M., Hennig, L., Kessler, F., Gruissem, W., and Baginsky, S. (2011). Plastid proteome assembly without Toc159: Photosynthetic protein import and accumulation of N-acetylated plastid precursor proteins. Plant Cell **23:** 3911–3928.

Buléon, A., Colonna, P., Planchot, V., and Ball, S. (1998). Starch granules: Structure and biosynthesis. Int. J. Biol. Macromol. **23:** 85–112.

Comparot-Moss, S., et al. (2010). A putative phosphatase, LSF1, is required for normal starch turnover in *Arabidopsis* leaves. Plant Physiol. **152:** 685–697.

Crevillén, P., Ventriglia, T., Pinto, F., Orea, A., Mérida, Á., and Romero, J.M. (2005). Differential pattern of expression and sugar regulation of *Arabidopsis thaliana* ADP-glucose pyrophosphorylase-encoding genes. J. Biol. Chem. **280:** 8143–8149.

Critchley, J.H., Zeeman, S.C., Takaha, T., Smith, A.M., and Smith, S.M. (2001). A critical role for disproportionating enzyme in starch breakdown is revealed by a knock-out mutation in *Arabidopsis*. Plant J. **26:** 89–100.

Delatte, T., Trevisan, M., Parker, M.L., and Zeeman, S.C. (2005). *Arabidopsis* mutants *Atisa1* and *Atisa2* have identical phenotypes and lack the same multimeric isoamylase, which influences the branch point distribution of amylopectin during starch synthesis. Plant J. **41:** 815–830.

Delatte, T., Umhang, M., Trevisan, M., Eicke, S., Thorneycroft, D., Smith, S.M., and Zeeman, S.C. (2006). Evidence for distinct mechanisms of starch granule breakdown in plants. J. Biol. Chem. **281:** 12050–12059.

Deschamps, P., et al. (2008). The heterotrophic dinoflagellate *Crypthecodinium cohnii* defines a model genetic system to investigate cytoplasmic starch synthesis. Eukaryot. Cell **7:** 872–880.

Faveri, S.B., and Vasconcelos, H.L. (2004). The Azteca-Cecropia association: Are ants always necessary for their host plants? Biotropica **36:** 641–646.

Fleming, T.H., and Williams, C.F. (1990). Phenology, seed dispersal, and recruitment in *Cecropia peltata* (Moraceae) in Costa Rican tropical dry forest. J. Trop. Ecol. **6:** 163–178.

Folgarait, P.J., Johnson, H.L., and Davidson, D.W. (1994). Responses of Cecropia to experimental removal of Mullerian Bodies. Funct. Ecol. **8:** 22–28.

Fulton, D.C., et al. (2008). Beta-AMYLASE4, a noncatalytic protein required for starch breakdown, acts upstream of three active beta-amylases in *Arabidopsis* chloroplasts. Plant Cell **20:** 1040–1058.

Geigenberger, P. (2011). Regulation of starch biosynthesis in response to a fluctuating environment. Plant Physiol. **155:** 1566–1577.

Götz, S., García-Gómez, J.M., Terol, J., Williams, T.D., Nagaraj, S.H., Nueda, M.J., Robles, M., Talón, M., Dopazo, J., and Conesa, A. (2008). High-throughput functional annotation and data mining with the Blast2GO suite. Nucleic Acids Res. **36:** 3420–3435.

Hussain, H., Mant, A., Seale, R., Zeeman, S., Hinchliffe, E., Edwards, A., Hylton, C., Bornemann, S., Smith, A.M., Martin, C., and Bustos, R. (2003). Three isoforms of isoamylase contribute different catalytic properties for the debranching of potato glucans. Plant Cell **15:** 133–149.

Kötting, O., Santelia, D., Edner, C., Eicke, S., Marthaler, T., Gentry, M.S., Comparot-Moss, S., Chen, J., Smith, A.M., Steup, M., Ritte, G., and Zeeman, S.C. (2009). STARCH-EXCESS4 is a laforin-like phosphoglucan phosphatase required for starch degradation in *Arabidopsis thaliana*. Plant Cell **21:** 334–346.

Kurtz, S., Phillippy, A., Delcher, A.L., Smoot, M., Shumway, M., Antonescu, C., and Salzberg, S.L. (2004). Versatile and open software for comparing large genomes. Genome Biol. **5:** R12.

Marshall, J.J., and Rickson, F.R. (1973). Characterization of the α-D-glucan from the plastids of *Cecropia peltata* as a glycogen-type polysaccharide. Carbohydr. Res. **28:** 31–37.

Meléndez, R., Meléndez-Hevia, E., Mas, F., Mach, J., and Cascante, M. (1998). Physical constraints in the synthesis of glycogen that influence its structural homogeneity: A two-dimensional approach. Biophys. J. **75:** 106–114.

Mortazavi, A., Williams, B.A., McCue, K., Schaeffer, L., and Wold, B. (2008). Mapping and quantifying mammalian transcriptomes by RNA-Seq. Nat. Methods **5:** 621–628.

Müller, F. (1876). Ueber das Haarkissen am Blattstiel der Imbauba (Cecropia), das Gemuesebeet der Imbauba-Ameise. Jenaische Zeitschrift fur Medizin und Naturwissenschaft **10:** 281–286.

Niittylä, T., Messerli, G., Trevisan, M., Chen, J., Smith, A.M., and Zeeman, S.C. (2004). A previously unknown maltose transporter essential for starch degradation in leaves. Science **303:** 87–89.

Patron, N.J., Waller, R.F., Archibald, J.M., and Keeling, P.J. (2005). Complex protein targeting to dinoflagellate plastids. J. Mol. Biol. **348:** 1015–1024.

Pérez-Guerrero, C., Herrera, M.D., Ortiz, R., Alvarez de Sotomayor, M., and Fernández, M.A. (2001). A pharmacological study of *Cecropia obtusifolia* Bertol aqueous extract. J. Ethnopharmacol. **76:** 279–284.

Rickson, F.R. (1971). Glycogen plastids in Mullerian Body cells of *Cecropia peltata* - A higher green plant. Science **173:** 344–347.

Rickson, F.R. (1976a). Anatomical development of leaf trichilium and Müllerian Bodies of *Cecropia peltata* L. Am. J. Bot. **63:** 1266–1271.

Rickson, F.R. (1976b). Ultrastructural differentiation of Müllerian Body glycogen plastid of *Cecropia peltata* L. Am. J. Bot. **63:** 1272–1279.

Robinson, M.D., McCarthy, D.J., and Smyth, G.K. (2010). edgeR: A Bioconductor package for differential expression analysis of digital gene expression data. Bioinformatics **26:** 139–140.

Robinson, M.D., and Oshlack, A. (2010). A scaling normalization method for differential expression analysis of RNA-seq data. Genome Biol. **11:** R25.

Roldán, I., Wattebled, F., Mercedes Lucas, M., Delvallé, D., Planchot, V., Jiménez, S., Pérez, R., Ball, S., D'Hulst, C., and Mérida, A. (2007). The phenotype of soluble starch synthase IV defective mutants of *Arabidopsis thaliana* suggests a novel function of elongation enzymes in the control of starch granule formation. Plant J. **49:** 492–504.

Saravanan, R.S., and Rose, J.K. (2004). A critical evaluation of sample extraction techniques for enhanced proteomic analysis of recalcitrant plant tissues. Proteomics **4:** 2522–2532.

Shearer, J., and Graham, T.E. (2002). New perspectives on the storage and organization of muscle glycogen. Can. J. Appl. Physiol. **27:** 179–203.

Streb, S., Delatte, T., Umhang, M., Eicke, S., Schorderet, M., Reinhardt, D., and Zeeman, S.C. (2008). Starch granule biosynthesis in *Arabidopsis* is abolished by removal of all debranching enzymes but restored by the subsequent removal of an endoamylase. Plant Cell **20:** 3448–3466.

Streb, S., Egli, B., Eicke, S., and Zeeman, S.C. (2009). The debate on the pathway of starch synthesis: A closer look at low-starch mutants lacking plastidial phosphoglucomutase supports the chloroplast-localized pathway. Plant Physiol. **151:** 1769–1772.

Streb, S., Eicke, S., and Zeeman, S.C. (2012). The simultaneous abolition of three starch hydrolases blocks transient starch breakdown in *Arabidopsis*. J. Biol. Chem. **287:** 41745–41756.

Sullivan, M.A., Vilaplana, F., Cave, R.A., Stapleton, D., Gray-Weale, A.A., and Gilbert, R.G. (2010). Nature of alpha and beta particles in glycogen using molecular size distributions. Biomacromolecules **11:** 1094–1100.

Szydlowski, N., et al. (2009). Starch granule initiation in *Arabidopsis* requires the presence of either class IV or class III starch synthases. Plant Cell **21:** 2443–2457.

Tomlinson, K., and Denyer, K. (2003). Starch synthesis in cereal grains. Adv. Bot. Res. **40:** 1–61.

Uchoa, V.T., de Paula, R.C., Krettli, L.G., Santana, A.E.G., and Krettli, A.U. (2010). Antimalarial activity of compounds and mixed fractions of *Cecropia pachystachya*. Drug Dev. Res. **71:** 82–91.

Usadel, B., Poree, F., Nagel, A., Lohse, M., Czedik-Eysenberg, A., and Stitt, M. (2009). A guide to using MapMan to visualize and compare Omics data in plants: A case study in the crop species, maize. Plant Cell Environ. **32:** 1211–1229.

Utsumi, Y., and Nakamura, Y. (2006). Structural and enzymatic characterization of the isoamylase1 homo-oligomer and the isoamylase1-isoamylase2 hetero-oligomer from rice endosperm. Planta **225:** 75–87.

Wang, R., et al. (2012). PRIDE Inspector: A tool to visualize and validate MS proteomics data. Nat. Biotechnol. **30:** 135–137.

Wattebled, F., Dong, Y., Dumez, S., Delvallé, D., Planchot, V., Berbezy, P., Vyas, D., Colonna, P., Chatterjee, M., Ball, S., and D'Hulst, C. (2005). Mutants of *Arabidopsis* lacking a chloroplastic isoamylase accumulate phytoglycogen and an abnormal form of amylopectin. Plant Physiol. **138:** 184–195.

Webber, B.L., Abaloz, B.A., and Woodrow, I.E. (2007). Myrmecophilic food body production in the understorey tree, *Ryparosa kurrangii* (Achariaceae), a rare Australian rainforest taxon. New Phytol. **173:** 250–263.

Yu, T.S., et al. (2001). The *Arabidopsis sex1* mutant is defective in the R1 protein, a general regulator of starch degradation in plants, and not in the chloroplast hexose transporter. Plant Cell **13:** 1907–1918.

Zeeman, S.C., Delatte, T., Messerli, G., Umhang, M., Stettler, M., Mettler, T., Streb, S., Reinhold, H., and Kotting, O. (2007). Starch breakdown: Recent discoveries suggest distinct pathways and novel mechanisms. Funct. Plant Biol. **34:** 465–473.

Zeeman, S.C., Kossmann, J., and Smith, A.M. (2010). Starch: Its metabolism, evolution, and biotechnological modification in plants. Annu. Rev. Plant Biol. **61:** 209–234.

Zeeman, S.C., Northrop, F., Smith, A.M., and Rees, T. (1998). A starch-accumulating mutant of *Arabidopsis thaliana* deficient in a chloroplastic starch-hydrolysing enzyme. Plant J. **15:** 357–365.

Zeeman, S.C., Tiessen, A., Pilling, E., Kato, K.L., Donald, A.M., and Smith, A.M. (2002). Starch synthesis in *Arabidopsis*. Granule synthesis, composition, and structure. Plant Physiol. **129:** 516–529.

Zerbino, D.R., and Birney, E. (2008). Velvet: Algorithms for *de novo* short read assembly using de Bruijn graphs. Genome Res. **18:** 821–829.

Zhang, X., Szydlowski, N., Delvallé, D., D'Hulst, C., James, M.G., and Myers, A.M. (2008). Overlapping functions of the starch synthases SSII and SSIII in amylopectin biosynthesis in *Arabidopsis*. BMC Plant Biol. **8:** 96.

Cecropia peltata Accumulates Starch or Soluble Glycogen by Differentially Regulating Starch Biosynthetic Genes

Sylvain Bischof, Martin Umhang, Simona Eicke, Sebastian Streb, Weihong Qi and Samuel C. Zeeman

Plant Cell 2013;25;1400-1415; originally published online April 30, 2013;
DOI 10.1105/tpc.113.109793